



Contents lists available at ScienceDirect

# Bioorganic & Medicinal Chemistry Letters

journal homepage: [www.elsevier.com/locate/bmcl](http://www.elsevier.com/locate/bmcl)

## I. Novel HCV NS5B polymerase inhibitors: Discovery of indole 2-carboxylic acids with C3-heterocycles

Gopinadhan N. Anilkumar\*, Charles A. Lesburg, Oleg Selyutin, Stuart B. Rosenblum, Qingbei Zeng, Yueheng Jiang, Tin-Yau Chan, Haiyan Pu, Henry Vaccaro, Li Wang, Frank Bennett, Kevin X. Chen, Jose Duca, Stephen Gavalas, Yuhua Huang, Patrick Pinto, Mousumi Sannigrahi, Francisco Velazquez, Srikanth Venkatraman, Bancha Vibulbhan, Sony Agrawal, Nancy Butkiewicz, Boris Feld, Eric Ferrari, Zhiqing He, Chuan-kui Jiang, Robert E. Palermo, Patricia Mcmonagle, H.-C. Huang, Neng-Yang Shih, George Njoroge, Joseph A. Kozlowski

Merck Research Laboratories, 2015 Galloping Hill Road, Kenilworth, NJ 07033, USA

### ARTICLE INFO

#### Article history:

Received 28 April 2011

Revised 30 June 2011

Accepted 6 July 2011

Available online 19 July 2011

#### Keywords:

HCV

NS5B polymerase

### ABSTRACT

SAR development of indole-based palm site inhibitors of HCV NS5B polymerase exemplified by initial indole lead **1** (NS5B  $IC_{50}$  = 0.9  $\mu$ M, replicon  $EC_{50}$  >100  $\mu$ M) is described. Structure-based drug design led to the incorporation of novel heterocyclic moieties at the indole C3-position which formed a bidentate interaction with the protein backbone. SAR development resulted in leads **7q** (NS5B  $IC_{50}$  = 0.032  $\mu$ M, replicon  $EC_{50}$  = 1.4  $\mu$ M) and **7r** (NS5B  $IC_{50}$  = 0.017  $\mu$ M, replicon  $EC_{50}$  = 0.3  $\mu$ M) with improved enzyme and replicon activity.

© 2011 Elsevier Ltd. All rights reserved.

Hepatitis C virus (HCV) is a major health hazard affecting over 170 million individuals worldwide<sup>1a</sup> and its infection is a leading cause of chronic liver cirrhosis and death from liver disease in the United States.<sup>1b,c</sup> The current standard of care is treatment with a combination of subcutaneous pegylated interferon administration with oral dosing of the cytotoxic nucleoside drug ribavirin.<sup>2</sup> The response rate is >75% for HCV patients with genotypes 2 and 3 after a 24 week treatment regimen while genotype 1 patients have a response rate of less than 50% after 48 weeks of treatment.<sup>3</sup> With a clear opportunity to improve clinical outcomes, and given the side effects associated with the current standard of care, it is valuable to discover potent inhibitors of HCV replication that will improve outcomes and shorten treatment duration.

The HCV NS5B protein is an RNA-dependent RNA polymerase critical for the synthesis of progeny viral genomes. The crystal structure of HCV NS5B displayed an overall subdomain architecture similar to other members of the Poll family,<sup>4</sup> with a deep active site cavity, located at the top of the 'palm' subdomain, and sealed at its base by a unique  $\beta$ -loop. Furthermore, there was an unexpected interaction identified between the tip of the 'fingers' subdomain and the 'thumb' subdomain to encircle the presumed nucleoside triphosphate substrate entry trajectory (Fig. 1).

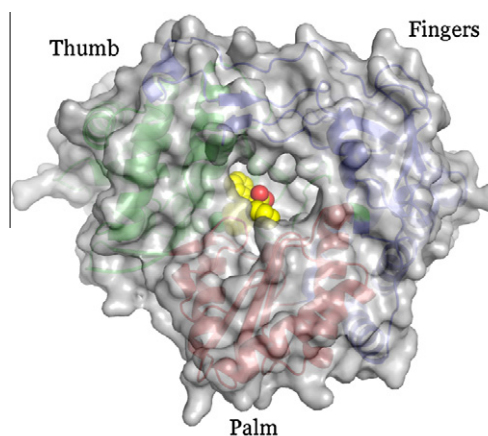


**Figure 1.** Overall protein molecular surface of NS5B with compound **1** (yellow spheres) bound within the active site cavity at the palm site. The 'fingers', 'palm', and 'thumb' domains are labeled and colored in blue, red, and green, respectively, beneath the molecular surface.

Sequence variation analysis suggests that residues lining the active site cavity ('palm site') more conserved than in other regions, such as the 'thumb-site'. This makes the palm site an attractive target for inhibition of the viral polymerase, though

\* Corresponding author.

E-mail address: [gopinadhan.anilkumar@merck.com](mailto:gopinadhan.anilkumar@merck.com) (G.N. Anilkumar).

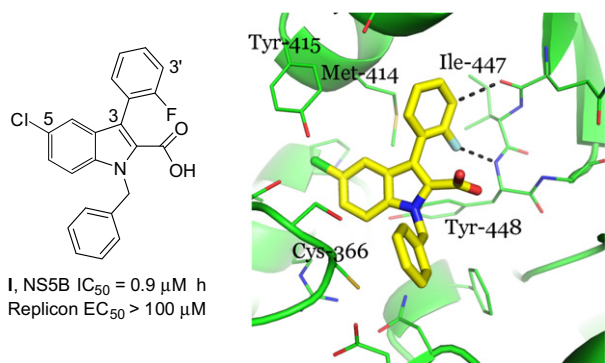


**Figure 2.** X-ray structure of lead indole acid analog **1** bound within the active site cavity of NS5B at the palm site. Residues presenting sidechain atoms within 5 Å of the compound are shown, along with backbone atoms of Ile-447 and Tyr-448. An unusual F...HN interaction and a close CH...O=C approach are illustrated by dotted lines.

not all residues lining this site are absolutely conserved. Clinical efficacy has been demonstrated with non-nucleoside inhibitors binding at the palm, thumb, and finger-loop subdomains.<sup>5</sup>

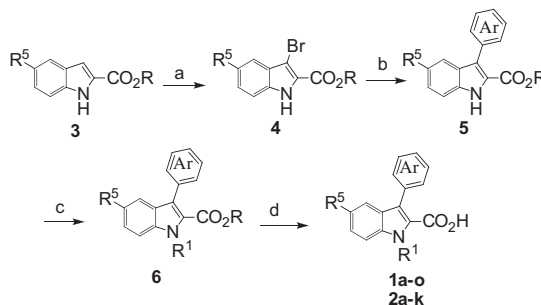
High throughput screening of HCV NS5B polymerase using a novel trinucleotide-primed assay,<sup>6</sup> designed to respond to both initiation and elongation inhibitors, revealed a structurally-similar cluster of weak indole inhibitors exemplified by initial lead **1** with ~0.9 μM binding affinity. The X-ray structure of NS5B with initial lead **1** (Fig. 2), confirms that compound **1** binds within the active site cavity of the apoprotein at the 'palm site'. The N-benzyl group of inhibitor **1** stacks upon Cys-366. The C2 carboxylate does not contact the protein directly. Hydrophobic interactions from the indole core and the N1 phenyl ring dominated the contacts, and make no specific polar interactions. The indole core and the C3 phenyl ring are in contact with the side chain of Met-414. Of particular note is the identification of an unusual F...HN interaction with a 2.6 Å distance between the C3 aromatic fluorine and the protein backbone of Tyr-448. The phenyl 3'-carbon adjacent to the fluorine is only 2.9 Å from the backbone carbonyl oxygen of Ile-447, well within the van der Waals contact distance. The indole 5-chlorine atom protrudes into a constricted tunnel formed primarily by hydrophobic and aromatic residues such as Leu-384 and Tyr-415.

The initial efforts were focused on variation of the indole N1 substituent with selected SAR is presented in Table 1. Synthesis of the analogs in Table 1 generally followed a route as outlined in Scheme 1. Commercially available indole 2-carboxylic acid esters (ethyl or methyl) were selectively brominated at the C3 position by treatment with N-bromosuccinimide. Bromide **4** was subjected to Suzuki coupling with aryl boronic acids using Pd(dppf)Cl<sub>2</sub> as the catalyst. N-alkylation of the indole was achieved by treatment with an appropriate halide and Cs<sub>2</sub>CO<sub>3</sub> as the base. It should be noted that other bases such as sodium hydride also gave satisfactory yields. In some examples the arylation and alkylation steps were done in a reverse order. In the final step, the indole C2 acids were prepared by hydrolysis of the corresponding ester using aqueous 1 N LiOH. In cases where there was no substitution at N1 (**1a**), the corresponding functionalization step was omitted.

The 5-chloro indole analog (**1a**) with an unsubstituted N1 was approximately 10-fold less potent than **1**, while introducing small alkyl substitutions like methyl at the N1 position were tolerated (**1b**). Both acetyl and benzoyl substitutions at the N1 position showed eightfold reduced enzyme activity (**1c,d**). Bulky lipophilic substitution such as naphthalene-2-ylmethyl was not tolerated (**1e**). The observed N1 SAR trend, coupled with the fact that the screening hits were part of a larger library with diverse N1 substitutions (not described), suggested the critical nature of the N1

**Table 1**  
Indole-N1 substitutions

Compds	R <sup>1</sup>	IC <sub>50</sub> (μM) <sup>7</sup>
<b>1</b>	Benzyl (lead)	0.9
<b>1a</b>	H	7.3
<b>1b</b>	Methyl	1.3
<b>1c</b>	Acetyl	8.1
<b>1d</b>	Benzoyl	7.8
<b>1e</b>	Naphthalene-2-ylmethyl	4.4
<b>1f</b>	3-Me-benzyl	2.5
<b>1g</b>	3-CF <sub>3</sub> -benzyl	>44
<b>1h</b>	3-CF <sub>3</sub> O-benzyl	1.8
<b>1i</b>	2,5-F-benzyl	0.3
<b>1j</b>	2-NH <sub>2</sub> -benzyl	0.6
<b>1k</b>	3-NH <sub>2</sub> -benzyl	0.2
<b>1l</b>	3-NH <sub>2</sub> , 4-Me-benzyl	1.3
<b>1m</b>	3-AcNH-benzyl	0.6
<b>1n</b>	3-BnNH-benzyl	0.7
<b>1o</b>	Pyridin-3-ylmethyl	1.3
<b>1p</b>	Pyridin-4-ylmethyl	1.2

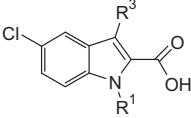


**Scheme 1.** General synthesis of analogs. Reagents and conditions: (a) NBS, THF, rt; (b) Ar-(B(OH)<sub>2</sub>), Pd(dppf)Cl<sub>2</sub>, K<sub>2</sub>CO<sub>3</sub>, H<sub>2</sub>O, DME, reflux; (c) R<sup>1</sup>-Br, Cs<sub>2</sub>CO<sub>3</sub>, DMF, rt; (d) aq 1 N LiOH, THF, reflux.

benzyl scaffold despite the lack of any obvious interaction with the protein. The focus was shifted to substitutions around the phenyl portion of the N1-benzyl group. The X-ray structure with **1**, showed that the benzyl group was close enough to the protein backbone that substitutions offered a chance to identify new interactions. Lipophilic benzyl substituents such as 3-methyl (**1f**), 3-trifluoromethyl (**1g**) and the 3-trifluoromethoxy analog (**1h**) were deleterious relative to the initial lead. On the other hand, 2,5-difluoro substitution of the benzyl group had a beneficial effect on the enzyme activity (**1i**, IC<sub>50</sub> = 0.3 μM). Both 2- and 3- amino substitutions also showed improved activity, with a regiochemical preference (**1j,k**, IC<sub>50</sub> = 0.6–0.2 μM) for 3-amino substituted benzyl. A follow up focused library of ~300 compounds with functionalized 3-amino substitutions to probe additional interactions with protein backbone did not identify any compounds with improved activity. The analogs which showed comparable activity to **1k** were the 3-acetyl and 3-amino benzyl analogs, **1m** and **1n**. The aniline liability of **1k** prompted preparation of pyridine-methyl analogs **1o** and **1p** which were equipotent with initial lead **1**.

The X-ray structure of the lead **1** revealed that the C3-fluoro-phenyl group is close to the protein backbone. Efforts were made to understand the potential interactions in this region as

**Table 2**  
Variation of C3-phenyl substitutions



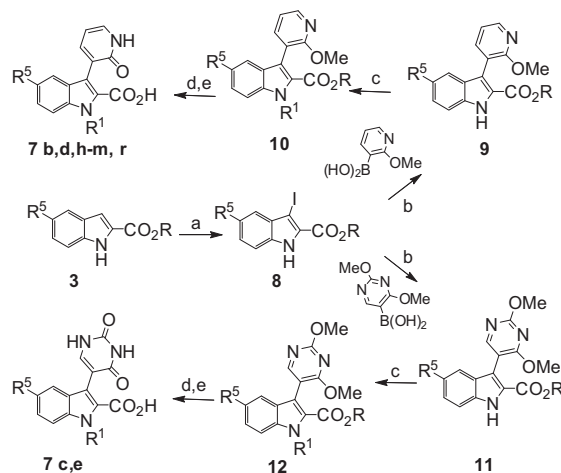
Compds	R <sup>1</sup>	R <sup>3</sup>	hIC <sub>50</sub> (μM) <sup>7</sup>
2a		H	17
2b			10
2c			1.4
2d			4.2
2e			33
2f			30
2g			29
2h			>48
2i			>46
2j			1.1
2k			0.3

summarized in Table 2. Syntheses of series 2a–k compounds were also achieved following the chemistry described in Scheme 1. Since halogen-substituted benzyl groups were tolerated at the indole N1 position, exemplified by 1i (IC<sub>50</sub> = 0.3 μM), both chloro- and fluoro-substituted benzyl analogs were installed at N1. The C3 unsubstituted indole analog (2a) was only a weak binder of NS5B. Replacement of fluorine at the *ortho* position of C3 phenyl with a methoxyl group attenuated activity as well (2b, IC<sub>50</sub> = 10 μM)

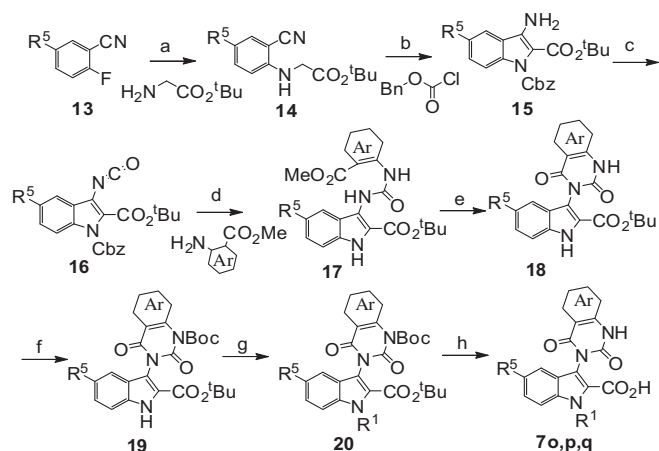
while hydroxyl substitution (2c, IC<sub>50</sub> = 1.4 μM) was tolerated. This observation suggested that this region does not accommodate bulky functionalities. Alternatively, an unsubstituted phenyl group at C3 (2d) also did not improve the binding activity, which suggested proper aromatic substitutions could have a positive impact on the binding with the protein. A variety of substitutions were examined at different positions around the C3-phenyl group as exemplified by 2e–j. Overall there was limited success in improving the binding activity. Apart from the observation that substitutions at 3- and 4- positions of the ring were not tolerated, it was noticed that the position of F group in the phenyl ring was also critical. This further reinforced the observation in the X-ray structure of 1 that *ortho* fluorine substitution is in close proximity with the Tyr-448 residue of the protein. The gain in activity from 2h (IC<sub>50</sub> = 48 μM to 2j (IC<sub>50</sub> = 1.1 μM) by adding in the 2'-F substituent is greater than 40-fold. Interestingly the 2'-fluoropyridine analog (2k, IC<sub>50</sub> = 0.3 μM) showed promising binding activity, but the observed chemical reactivity of this system raised questions about the stability and selectivity which deprioritized further follow up.

Our initial efforts to explore the N1 and C3 positions of the lead compound 1 resulted in many compounds with sub-micromolar enzyme activity (IC<sub>50</sub> = 0.2–0.3 μM). None of these compounds showed significant cell based activity in the replicon assay (EC<sub>50</sub> > 25 μM). This prompted us to revisit the X-ray structure of the lead compound 1 and look for specific interactions with protein which can be improved. The most obvious finding from the X-ray structure as described above was the F...HN interaction. We reasoned that this may be an interaction with the protein which can be improved if we can replace the C-F with a carbonyl, as a C=O...HN would provide a more canonical hydrogen bonding interaction. Thus analogs with carbonyl containing functionalities were targeted. The synthesis of diverse N-linked and C-linked heterocycles at the indole C3 position were carried out as described in Schemes 2–4.

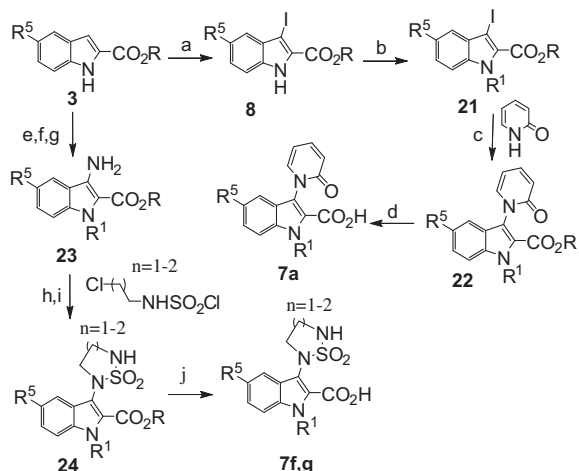
Synthesis of the C-linked heterocyclic analogs pyridone and pyrimidinedione in Table 3 were made as outlined in Scheme 2. The indole 2-carboxylic acid esters (ethyl or methyl) were selectively iodinated at the C3 position by treatment with *N*-iodosuccinimide. The 3-iodo intermediate 8 was subjected to Suzuki coupling with either 2-methoxyphenyl boronic acid or 2,4-dimethoxyphenyl boronic acid using Pd(dppf)Cl<sub>2</sub> as the catalyst. The subsequent N-alkylation of the indole was achieved with an appropriate electrophile, and typically using Cs<sub>2</sub>CO<sub>3</sub> as the base.



**Scheme 2.** General synthesis of C3- C-linked hetero analogs. Reagents and conditions: (a) NIS, CHCl<sub>3</sub>, rt; (b) Pd(dppf)Cl<sub>2</sub>, K<sub>2</sub>CO<sub>3</sub>, H<sub>2</sub>O, DME, reflux; (c) R<sup>1</sup>-Br, Cs<sub>2</sub>CO<sub>3</sub>, DMF, rt; (d) 4 N HCl/dioxane, MeOH, 90 °C; (e) aq 1 N LiOH, TFH, reflux.



**Scheme 3.** General synthesis of C3 N-linked pyrimidinediones. Reagents and conditions: (a) DIEA, NMP, 110 °C; (b) KOtBu, THF, DMF, rt; (c) triphosgene, TEA, Toluene, reflux; (d) trifluoromethylbenzene, microwave, 150 °C; (e) NaOMe, MeOH, microwave, 100 °C; (f) (Boc)<sub>2</sub>O, Dioxane, rt; (g) R1-Br, KOtBu, THF, DMF, rt; (h) TFA, DCM, rt.



**Scheme 4.** General synthesis of C3 N-linked pyridone and sulfonyl urea. Reagents and conditions: (a) NIS, CHCl<sub>3</sub>, rt; (b) R1-Br, Cs<sub>2</sub>CO<sub>3</sub>, DMF, rt; (c) CuI, K<sub>2</sub>CO<sub>3</sub>, 8-hydroxyquinoline, DMSO, 100 °C; (d) aq LiOH, THF, reflux.; (e) nitric acid, (f) R<sup>1</sup>-Br, Cs<sub>2</sub>CO<sub>3</sub>, DMF, rt; (g) H<sub>2</sub>, Pd-C; (h) Et<sub>3</sub>N; (i) Cs<sub>2</sub>CO<sub>3</sub>, (j) aq LiOH, THF.

The reverse sequence of functionalizing N1 and C3 was also used in some examples. The demethylation of intermediates **10** and **12** with 4 N HCl in dioxane liberated the pyridone and pyrimidinedione moieties at C3 position. As above the final C2 ester hydrolysis step was accomplished by use of aqueous LiOH.

Analogs with N-linked pyrimidinediones were synthesized as described in Scheme 3 below. The 3-amino indole intermediate **15** was prepared in two steps from 2-fluorobenzonitrile **13**. Intermediate **15** was converted to the C3-isocyanate **16** with triphosgene, which was subsequently treated with appropriate aromatic *ortho*-amino esters to form urea derivatives **17**. Intermediate **17** was cyclized to the pyrimidinedione analog **18** by heating with sodium methoxide. Subsequent protection, N-alkylation and deprotection steps under standard conditions yielded the final compounds **7o–q**.

The syntheses of N-linked pyridone and cyclic sulfonyl urea derivatives at C3 were accomplished as described in Scheme 4. The key reaction step for synthesis of N-linked pyridone analog was the copper iodide mediated N-arylation of intermediate **21** to **22**. The cyclic sulfonyl urea derivatives were synthesized from

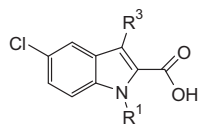
3-aminoindole **23** which was cyclized to **24** under basic conditions by reaction with corresponding chloro alkyl sulfamoyl chlorides.

Earlier SAR results at N1 demonstrated that either fluoro- or amino- substituted benzyl groups were preferred. These particular N1-benzyl groups were selected for further SAR explorations (Table 3). Interestingly, the N-linked pyridone analog **7a** showed an improved enzyme potency with moderate replicon activity (IC<sub>50</sub> = 0.15 μM, EC<sub>50</sub> = 19 μM). The X-ray structure with lead compound **1** had also revealed a close contact between the hydrogen at *meta* position of the C3 phenyl and the carbonyl group of Ile-447. This suggested an opportunity to replace this interaction with a N-H...O=C, which could result in bidentate interaction of the inhibitor with the protein backbone. To achieve such an interaction, the C-linked pyridone derivative **7b** was prepared which could offer the desired C=O and NH functionalities needed to interact with the polypeptide backbone of Tyr-448 and Ile-447. Gratifyingly, **7b** showed a substantial improvement in the enzyme activity (IC<sub>50</sub> = 35 nM) and moreover an improved replicon activity (EC<sub>50</sub> = 10 μM). The discovery of the pyridone moiety at C3 which anchored the inhibitor in the active site cavity of the enzyme encouraged us to look for other similar functionalities in this region. A pyrimidinedione derivative **7c** also displayed enzyme and replicon activity comparable to the pyridone. The N1 aminobenzyl group showed a positive impact on the binding activity from earlier SAR (**11**), but presented a potential aniline toxicology liability, the corresponding aminopyridylmethyl analogs were prepared at N1. Both C3 pyridone and pyrimidinedione analogs in this series (**7d,e**) showed improved replicon activity while maintaining similar enzyme potency (EC<sub>50</sub> = 2–4.8 μM). Five- and six-membered sulfonyl urea analogs (**7f,g**) were both inactive, suggesting improper alignment of the interacting groups.

The chloro group at R<sup>5</sup> position protruded into a constricted tunnel defined by primarily lipophilic residues as seen in the X-ray. A limited effort to fine-tune the C5 functionality in the pyridone series (**7h–m**) showed intolerance to bulky groups while small alkyls and halogens were preferred. The trifluoromethyl analog at this position showed comparable binding affinity with an improved replicon activity (**7m**, EC<sub>50</sub> = 4.8 μM) to the 5-chloro compound **7b** (EC<sub>50</sub> = 10 μM). Further efforts to improve the cell based activity in this series were performed with a C5 trifluoromethyl group. The decreased enzyme activity of acyclic urea derivative **7n** (IC<sub>50</sub> = 0.35 μM) highlighted the importance of proper alignment the amide pairs of the inhibitor and protein to evoke the bidentate interaction to anchor the molecule. Efforts to construct a stable cyclic structure which could align this urea moiety properly were successful with the reverse pyrimidinedione analogs **7o,p**. For example, the thienopyrimidinedione (**7p**, IC<sub>50</sub> = 59 nM, EC<sub>50</sub> = 12 μM) showed the best activity profile. Since the C5 trifluoromethyl group showed improved replicon activity, we wanted to examine the effect this could provide in combination with the N1 aminopyridylmethyl group. Gratifyingly both the thienopyrimidinedione (**7q**, IC<sub>50</sub> = 32 nM, EC<sub>50</sub> = 1.4 μM) and pyridone (**7r**, IC<sub>50</sub> = 17 nM, EC<sub>50</sub> = 0.3 μM) analogs in this series showed greatly improved enzyme and cell based activity. The pyridone analog **7r** was the first compound in this series to afford sub-micromolar replicon activity.

X-ray structures of representative inhibitors with C3-heterocycles designed to have improved backbone interactions were observed to bind to the active site of the enzyme (Fig. 3). These compounds exhibited the intended interactions with the backbone atoms of Ile-447 and Tyr-448. Furthermore, the optimal aminopyridylmethyl group was found to interact with the sidechain hydroxyl of Ser-367 and the C2-carboxylate group interacted with the protein backbone at Gly-449 indirectly via a bridging water molecule.

**Table 3**  
Variation of C3 hetero substitutions



Compds	R <sup>5</sup>	R <sup>1</sup>	R <sup>3</sup>	IC <sub>50</sub> (μM) <sup>7</sup>	EC <sub>50</sub> (μM) <sup>8</sup>
7a	Cl			0.15	19
7b	Cl			0.035	10
7c	Cl			0.047	10
7d	Cl			0.053	4.8
7e	Cl			0.031	2.0
7f	Cl			>20	NA
7g	Cl			>20	NA
7h	Br			0.043	7.6
7i	OMe			0.043	11
7j	OEt			0.12	20
7k				0.56	>50
7l	Me			0.046	Cytotox@5 μM
7m	CF <sub>3</sub>			0.025	4.8
7n	CF <sub>3</sub>			0.35	>10

Table 3 (continued)

Comps	R <sup>5</sup>	R <sup>1</sup>	R <sup>3</sup>	IC <sub>50</sub> (μM) <sup>7</sup>	EC <sub>50</sub> (μM) <sup>8</sup>
<b>7o</b>	CF <sub>3</sub>			0.27	>10
<b>7p</b>	CF <sub>3</sub>			0.059	12
<b>7q</b>	CF <sub>3</sub>			0.032	1.4
<b>7r</b>	CF <sub>3</sub>			0.017	0.3

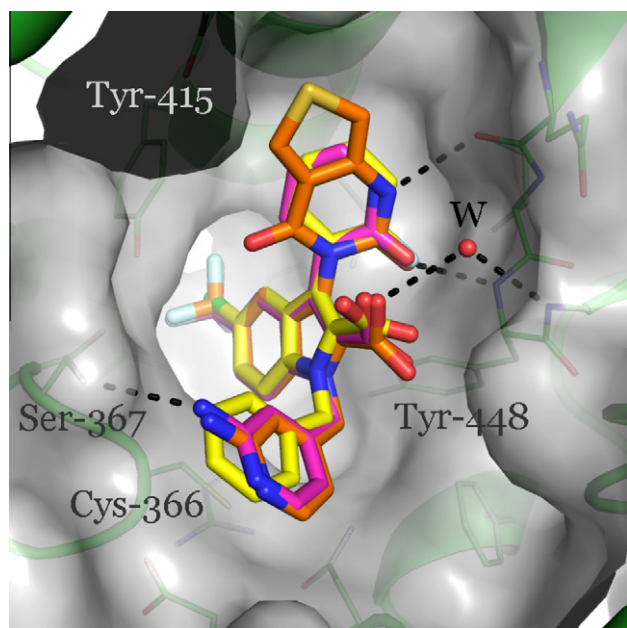


**Figure 3.** X-ray structures of complexes with C3-heterocycles (orange: **7q**; magenta: **7r**) superimposed upon the structure of NS5B complexed with **1** (yellow) [9,10]. In the structures containing a C3 heterocycle, a water molecule was observed (denoted 'W') which bridges the C2 carboxylate group and the backbone NH group of Gly-449. The N1-aminopyridyl group interacts with the sidechain hydroxyl of Ser-367.

In conclusion, we have described a structure-based drug design assisted progression of a low affinity indole lead **1** with no detectable replicon activity to advanced leads with nanomolar NS5B enzyme potency and sub-micromolar replicon activity. The X-ray structure of initial lead **1** in the palm site of NS5B suggested potential hydrogen bonding interactions with the protein backbone. Directed SAR investigations to maximize the bidentate backbone interactions led to the discovery of heterocyclic moieties such as

C3 pyridone **7r** and pyrimidinedione **7q**. Further optimization efforts in this series will be reported in separate publications.

#### References and notes

- (a) Cohen, J. *Science* **1999**, 285, 26; (b) Alter, M. J.; Kruszon-Moran, D.; Nainan, O. V.; McQuillan, G. M.; Gao, F.; Moyer, L. A.; Kaslow, R. A.; Margolis, H. S. *N. Engl. J. Med.* **1999**, 341, 556; (c) Cuthbert, J. A. *Clin. Microbiol. Rev.* **1994**, 7, 505; (d) Monto, A.; Wright, T. L. *Semin. Oncol.* **2001**, 441.
- (a) Neumann, A. U.; Lam, N. P.; Dahari, H.; Gretch, D. R.; Wiley, T. E.; Layden, T. J.; Perelson, A. S. *Science* **1998**, 282, 103; (b) Rosen, H. R.; Gretch, D. R. *Mol. Med. Today* **1999**, 5, 393; (c) Di Bisceglie, A. M.; McHutchison, J.; Rice, C. M. *Hepatology* **2002**, 35, 224.
- Zeuzem, S.; Berg, T.; Moeller, B.; Hinrichsen, H.; Mauss, S.; Wedemeyer, H.; Sarrazin, C.; Hueppe, D.; Zehnter, E.; Manns, M. P. *J. Viral Hepat.* **2009**, 16, 75.
- (a) Lesburg, C. A.; Cable, M. B.; Ferrari, E.; Hong, Z.; Mannarino, A. F.; Weber, P. C. *Nat. Struct. Biol.* **1999**, 6, 937; (b) Bressanelli, S.; Tomei, L.; Roussel, A.; Incitti, I.; Vitale, R. L.; Mathieu, M.; De Francesco, R.; Rey, F. A. *Proc. Natl. Acad. Sci. U.S.A.* **1999**, 96, 13034.
- Beaulieu, P. L. *Expert Opin. Ther. Pat.* **2009**, 19, 145.
- (a) Ferrari, E.; He, Z.; Palermo, R. E.; Huang, H. C. *J. Biol. Chem.* **2008**, 283, 33893; (b) Cheng, C. C.; Shipps, G. W., Jr.; Yang, Z.; Kawahata, N.; Lesburg, C. A.; Duca, J. S.; Bandouveres, J.; Bracken, J. D.; Jiang, C. K.; Agrawal, S.; Ferrari, E.; Huang, H. C. *Bioorg. Med. Chem. Lett.* **2010**, 20, 2119.
- HCV NS5B polymerase activity was measured in a radiolabeled nucleotide incorporation assay as described [Cheng 2010], in a reaction buffer containing 20 mM HEPES (pH 7.3), 7.5 mM DTT, 20 U/mL RNasin, 0.1 μM GTP, ATP and UTP, 60 μCi/ml [<sup>33</sup>P]-CTP supplemented to 20 nM CTP, 10 mM MgCl<sub>2</sub>, 60 mM NaCl, 100 μg/ml BSA, 100 nM heteropolymer RNA template, 0.25 mM trinucleotide initiator and 30 nM NS5B (Δ21) enzyme. Reaction was allowed to proceed for 150 min at room temperature and terminated by EDTA. The reaction mixture was washed on Millipore DE81 filter plate and the incorporated labeled CTP quantitated by Packard TopCount. Compound IC<sub>50</sub> values were calculated from experiments with 10 serial twofold dilutions of the inhibitor in duplicate.
- To measure cell-based anti-HCV activity, replicon cells (1b-Con1) were seeded at 5000 cells/well in 96-well plates one day prior to inhibitor treatment. Various concentrations of an inhibitor in DMSO were added to the replicon cells, with the final concentration of DMSO at 0.5% and fetal bovine serum at 5% in the assay media. Cells were harvested 3 days post dosing. The replicon RNA level was measured using real-time RT-PCR (Taqman assay) with GAPDH RNA as endogenous control. EC<sub>50</sub> values were calculated from experiments with 10 serial twofold dilutions of the inhibitor in duplicate.
- Figures 1–3 were generated using the program PyMOL (The PyMOL Molecular Graphics System, Version 1.2r1, Schrödinger, LLC).
- Crystal structures of HCV NS5B in complex with **1**, **7r**, and **7q** have been deposited in the Protein Data Bank with accession numbers 3SKH, 3SKE, 3SKA, respectively.